Journal of Archaeological Science 90 (2018) 62–70

Contents lists available at ScienceDirect

Journal of Archaeological Science

journal homepage: http://www.elsevier.com/locate/jas

Quantifying the effects of erosion on archaeological sites with low-altitude aerial photography, structure from motion, and GIS: A case study from southern Jordan

Matthew D. Howland [a, b, *], Ian W.N. Jones [a, b], Mohammad Najjar [b], Thomas E. Levy [a, b]

[a] Center for Cyber-Archaeology and Sustainability, Qualcomm Institute, University of California, Atkinson Hall, 9500 Gilman Drive, La Jolla, San Diego, CA, 92093, USA
[b] Department of Anthropology, University of California, Social Sciences Building Room 210, 9500 Gilman Drive, La Jolla, San Diego, CA, 92093-0532, USA

ARTICLE INFO

Article history:
Received 26 September 2016
Received in revised form
30 November 2017
Accepted 26 December 2017

Keywords:
Site formation processes
Erosion
GIS
SfM
IBM
Balloon aerial photography

ABSTRACT

Cutting-edge photogrammetric techniques combined with traditional methods are a boon for archaeologists interested in performing spatial analyses. Low-altitude aerial photography (LAAP) combined with photogrammetric Image Based Modeling (IBM) comprise a workflow that allows for precise and accurate recording of both photographic and elevation data of archaeological sites with a great deal of speed and efficiency. Through these techniques, the researcher can create spatially-referenced orthophotos and digital elevation models (DEMs), which can serve as the basis for investigations into site formation processes. Due to the rapidity of the creation of these datasets, analysis of site formation processes can be completed over the course of hours or days. The results of such site formation studies can inform and guide further archaeological investigations of sites. This paper presents the application of a combined LAAP-IBM method to acquire GIS data, which serves as the basis for a case study of a new model of the effects of erosion on archaeological sites – a key factor in understanding site formation processes. These methods are applied to Khirbat Nuqayb al-Asaymir, a Middle Islamic site in southern Jordan, as a case study.

1. Introduction

The process of archaeology relies on interpreting how things were in the past (the systemic context) from how things are in the present (the archaeological context) (Schiffer, 1972). This, in turn, depends on the correction of distortions caused by cultural and environmental formation processes (c- and n-transforms, respectively), affecting the archaeological record after the original deposition of artifacts. Fortunately, formation processes have predictable and discoverable effects on the archaeological record, an area of theory that has been developed by Michael B. Schiffer (1972: 678), meaning that these transformations can be understood and accounted for. The documentation of biases caused by formation processes facilitates the reconstruction of the relationship between systemic and archaeological contexts. However, archaeological research relies on the existence of empirical evidence in order to demonstrate that certain n-transforms occurred. This is an *a posteriori* approach to making inferences about natural transformation processes' effects on the archaeological record (See Cruz et al., 2014 for an excellent example of one such study). We suggest here that certain ubiquitous environmental transformation processes do not need to be proven to have occurred before they are considered in archaeological research, given the likelihood of their occurrence. As such, *a priori* presupposition of these factors may provide insight into the predictable patterns of evidence one would expect to find as the results of these processes when conducting intensive archaeological investigation. In the same way that one would be unlikely to plan excavation or survey without due consideration of the ways in which cultural formation processes (i.e. artifact deposition) affect the archaeological record, we propose that the biasing effects of environmental formation processes such as erosion are also important to factor into planned investigation of archaeological sites. Erosion in particular has rarely been the main focus of comprehensive archaeological study, with some exceptions (James et al., 1994; Stiros et al., 1999; Turnbaugh, 1978; chapters in

* Corresponding author. UC San Diego, Department of Anthropology, 9500 Gilman Drive, #0532, La Jolla, CA 92093-0532, USA.
E-mail address: mdhowlan@ucsd.edu (M.D. Howland).

https://doi.org/10.1016/j.jas.2017.12.008
0305-4403/

Meylemans et al., 2014). Attempts to develop a general model specifically aimed at estimating the distortions in spatial patterning of artifacts caused by erosion at various sites (e.g. Wainwright, 1994) are even more rare. In our view, such a model can provide substantial benefits in terms of understanding the spatial distribution of artifacts at sites prone to erosion.

Fortunately, recent developments in field recording methods and technology provide an excellent basis for an *a priori* study of water-caused erosion at archaeological sites. We have developed a workflow using techniques including low-altitude aerial photography, computer vision, soil science, ethnoarchaeology, and GIS to study the effects of this formation process. Our aims in conducting this work are threefold: first, we intend to demonstrate the viability of conducting various spatial analyses usually applied at a regional level at an intra-site scale. Second, we develop a model workflow for detailed site survey and *a priori* consideration of erosion as a site formation process affecting the development of archaeological context. Finally, we apply these studies to the site of Khirbat Nuqayb al-Asaymir (henceforth KNA) (Fig. 1), a copper production site in southern Jordan's Faynan region dating to the Middle Islamic Ic-IIa (ca. 2nd half of 12th to 1st half of 13th century CE) periods (Jones et al., 2012, 2014, 2017), for use in understanding the spatial distribution of artifacts and the relationship between systemic and archaeological context at the site.

2. Materials and methods

2.1. Low-altitude aerial photography and structure from motion

During the 2012 and 2014 UC San Diego Edom Lowlands Regional Archaeological Project (ELRAP) expeditions to the Faynan region of southern Jordan, the team developed an integrated workflow for detailed aerial archaeological survey (Fig. 2).

ELRAP deployed a low-altitude aerial photography (LAAP) photography platform for the purposes of photogrammetric Image-based modeling-oriented data collection and three-dimensional spatial survey of investigated sites in the region. Image-based modeling (IBM) is a broad term for the use of 2D images to generate 3D representations of physical objects (Remondino and El-Hakim, 2006: 271). One increasingly popular digital approach to IBM, Structure from Motion (SfM), applies photogrammetric principles to digital photographs in order to generate a 3D point cloud. SfM processes identify “feature points” (matching pixels) across multiple photographic images through comparison of their intensity and the characteristics of their geometric neighborhood. These points, along with Exif data (metadata describing the camera settings and other information about each image), allow for the

Fig. 1. Khirbat Nuqayb al-Asaymir. The varied topography of the site is clear in this image.

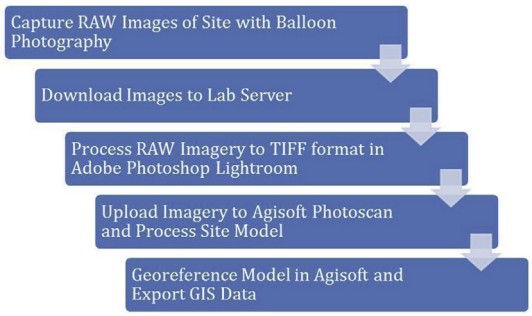

Fig. 2. ELRAP's integrated workflow for detailed aerial archaeological survey.

algorithm to calculate the relative locations from which each photo used in processing was taken and to form a sparse point cloud (Ullman, 1979). Many software packages released in recent years (including Agisoft Photoscan, http://www.agisoft.com/, one particularly popular application) combine SfM-based point cloud generation with mesh model and texture generation functions, for an integrated IBM workflow. Archaeologists have noted the cost-effectiveness of these digital photogrammetric techniques, their precision and accuracy (in some cases rivaling laser scanning), and its temporal efficiency in field recording (Verhoeven, 2011; Doneus et al., 2011: 84; Lambers et al., 2007; De Reu et al., 2014; Quartermaine et al., 2014; Forte, 2014: 13; Roosevelt, 2014; Meylemans et al., 2014; Jorayev et al., 2016; Reshetyuk and Mårtensson, 2016; Sapirstein, 2016; Thomas.,). Others have highlighted the capacity of photogrammetric IBM techniques for documentation at many scales, ranging from the artifact-to the site-level (Olson et al., 2013). IBM-oriented photographic data collection can allow for the production of high-quality spatial datasets suitable for interpretation and analysis within a Geographic Information System (GIS) framework at levels of resolution and accuracy unparalleled by other techniques (Howland, 2014: 106). The GIS-compatible datasets produced through IBM-based approaches consist of digital elevation models (DEMs) and orthophotographs, vertical photographs corrected for lens and elevation distortions (Howland, 2014; Verhoeven et al., 2012). The technique can also be married to methods of low-altitude aerial photography to expand the scale of data collection to a site-wide or greater extent (Verhoeven, 2011; Olson et al., 2013; Remondino et al., 2011; Howland, 2014; Smith et al., 2014; Roosevelt, 2014; Sapirstein, 2016; Jorayev et al., 2016). Given the possibility of rapid collection of accurate, precise, and useful 3D and spatial data through combined LAAP and IBM approaches, these methods form an excellent basis for preliminary survey of archaeological sites.

To perform this type of aerial 3D survey, ELRAP deployed a 1-ply Kingfisher Aerostat K14U-SC balloon (Dimensions: ca. 3.6 m × 3.0 m, volume: ca. 21.0 m^3, and lift: ca. 13.6 kg when fully inflated, tethered with 800lb SPECTRA line) tethered to and manipulated by a ground-based operator. This balloon was outfitted with a custom triangular frame capable of holding one or two high-resolution (15.1 megapixel) Canon EOS 50D Digital Single-Lens Reflex (DSLR) cameras equipped with 18 mm lenses. The balloon was selected over other LAAP options (such as UAVs or kites) due to the stability of the platform, its greater net lift, and the reduced chance of a catastrophic crash. The balloon also had performed well in prior field expeditions for similar purposes (Smith et al.2015; Howland, 2014). This platform allowed for an intensive campaign of photographic and 3D recording during the ELRAP field season.

The team intensively photographed five relatively large sites (Neolithic Wadi Fidan 61 [ca. 6ha] Levy et al., 2001), the Iron Age

sites Khirbat al- Ghuwayba [ca. 7ha] (Levy et al., 2003), Khirbat en-Nahas [ca. 10ha] (Levy et al., 2014c), and Khirbat al-Jariya [ca. 7ha](Ben-Yosef et al., 2010), and Middle Islamic Ic-IIa KNA [ca. 8ha] (Jones et al., 2012) (the subject of this paper) using the balloon platform (Howland, 2014). These sites have been intensively investigated by ELRAP as part of the project's deep-time study of metallurgical technology and social evolution (Levy et al., 2014b). Image acquisition at KNA consisted of the collection of 361 images captured at ca. 100 m elevation, with ca. 75% overlap between adjacent images. All data acquired at KNA were processed through the commercially-available software package Agisoft Photoscan. Precise details regarding image capture and the 3D model processing workflow within Agisoft Photoscan on the ELRAP project have been published elsewhere (Howland, 2014; Howland et al., 2015) and do not bear repeating here beyond a brief elaboration on the resolution and spatial accuracy of the KNA model. The sitewide model was georeferenced based on 12 easily identifiable control points, marked across the site with spray paint, and recorded with a Leica Flexline TS02 Plus total station. We estimate the accuracy of these points to be approximately ± 3 cm, given the inherent accuracy parameters of the total station itself and the nature of the control points. The model's spatial error, as reported by Agisoft, was 11.54 cm, referring to the RMSE of the ground control points identified in the images and their locations in the produced model. This number indicates that the geometry of the model has some distortions causing a level of spatial error in the model that is not ideal. However, we consider it to be well within acceptable limits when considered within the context of a sitewide study of erosion, which is necessarily imprecise. More localized models with far smaller error levels more suited to rock drawing were also captured at the site in cases where higher accuracy was needed. The sitewide model of KNA was ultimately used to generate an orthophotograph at 2 cm resolution and a digital elevation model (DEM) with 5 cm resolution of the site. These datasets produced through these methods have significantly better accuracy and resolution than other available data, which is usually satellite-derived.

2.2. Quantifying erosion

These GIS outputs serve as an excellent basis for forms of analysis not possible without such high resolution data, including a detailed investigation into erosion at archaeological sites—the focus of this paper. Our approach to this investigation is twofold. We have attempted to both quantify erosion risk and predict the spatial patterning of eroded material. Both of these procedures rely on GIS data produced through ELRAP's LAAP and IBM campaign, as well as data and methods drawn from other sources. To estimate the risk of erosion at archaeological sites and at KNA in particular, we have applied the Revised Universal Soil Loss Equation (RUSLE), a formula created (Wischmeier and Smith, 1965) and later revised (Renard et al., 1994) by the United States Department of Agriculture and often applied by soil scientists to calculate rates of rain-caused erosion on plots of land or specific field areas (Wischmeier and Smith, 1978: 3; Yoon et al., 2009). RUSLE, in other words, predicts annual rates of erosion over long periods of time. RUSLE was selected from among several erosion modeling methods (such as WEPP, USPED, etc) due to the formula's (relative) simplicity, the ease of acquiring necessary data to perform the relevant calculations, and the formula's compatibility with GIS-based analysis (Ganasri and Ramesh, 2016: 955). RUSLE has been described as the most practical erosion model for use at the local level, and can be appropriately applied at scales of less than 10 ha, which—though medium-sized for an archaeological site—is small by the agricultural standards on which many soil studies are based (Ganasri and Ramesh, 2016: 956; Taguas et al., 2010). That hyperspecific variables are not necessary for the equation was also an important consideration, due to the lack of readily available soil and climatic data for the study area. Importantly, RUSLE does not account for soil deposition, only rates of erosion (Chen et al., 2008). Furthermore, the equation does not consider erosion caused by wind, gravity, or even streams, meaning the current study is not a comprehensive study of all erosion processes at the site. Another consideration is that RUSLE is a formula designed with regard to naturally forming and occurring soil profiles. Thus it is important for this study to distinguish between these and anthropogenic deposits with associated natural sedimentation. The latter deposits we refer to as "sediment," reflecting the absence of natural soil horizons and profiles. This study will reflect our assumption that all deposits at the site have been subject to anthropogenic modification and as such should be characterized as sediment (rather than soil). Thus, this paper will apply RUSLE to address the rain-based erosion of sediment at KNA.

The RUSLE calculation requires five variables describing the conditions in the area in which one wishes to calculate erosion in tonnes/hectare/year (A), which are multiplied together (Fig. 4).

These are the *rainfall erosivity factor (R)*, a measure of the degree to which local conditions of precipitation cause erosion, the *soil erodibility factor (K)*, which relates to the potential of the soil to erode, the *length-slope factor (LS)*, which accounts for the influence of topography, and *cropping (C)* and *conservation practice (P)* factors, which relate to the effects of vegetation and slope, respectively, on erosion (Goldman et al., 1986: 5.2). We collected the data required to calculate each of these variables for KNA from a number of sources. The precipitation data needed for the computation of the R-factor was obtained from Hijmans et al (2005), allowing us to approximate the variable using Renard and Freimund (1994: 299) equation ($R = 0.0483P^{1.610}$, where P = an annual precipitation total less than 850 mm) for low-precipitation areas—resulting in an R of 46.182 (unitless) across the site of KNA. The type of detailed soil survey data required to estimate the K-factor for sediments at KNA was not readily available and not measured in the field due to a lack of the expertise and equipment needed for exact soil classification. As such, we were forced to rely on proxy data acquired from a soil profile (Casler, 2006) from land approximately 5.5 km to the south, though still in the Faynan region. Though it would be preferable to apply information from data directly from the site, the near-absence of soil data in Jordan requires that a somewhat wider net be cast (the present study would be improved somewhat if resources and funding for a detailed local soil survey were available). Because of these shortcomings, calculating the sediment erodibility factor required some estimations within the bounds of the data that was included in the soil survey; specifically the exact texture composition of the sediment in terms of percentage of sand, silt, and clay making up the sediment, beyond its characterization as a silty clay loam. The values were estimated as follows: particle size parameter ≈3575, percent organic matter ≈0.5, soil structure index ≈2, profile-permeability class factor ≈5, percent clay ≈35. Applying these approximations, we calculated a (unitless) K-factor of 0.520 using the formula ($K_{fact} = (1.292)[2.1 \times 10^{-6}\ f_p^{1.14}\ (12 - P_{om}) + 0.0325(S_{struc} - 2) + 0.025(f_{perm} - 3)]$, with a modifying factor of 0.105 added based on the estimated organic matter content of 0.5%), the mathematical representation of the nomograph provided by Wischmeier et al. (1971), which we regard as a rough but suitably accurate approximation of the variable's actual value. K-factor for this study is considered as a sitewide constant due to the relatively small size of the site and lack of identifiable variation in sediment across the site. The LS-factor was a more precise calculation as it is possible to derive the data needed to calculate this variable from a DEM using functions within ArcGIS. The LS-

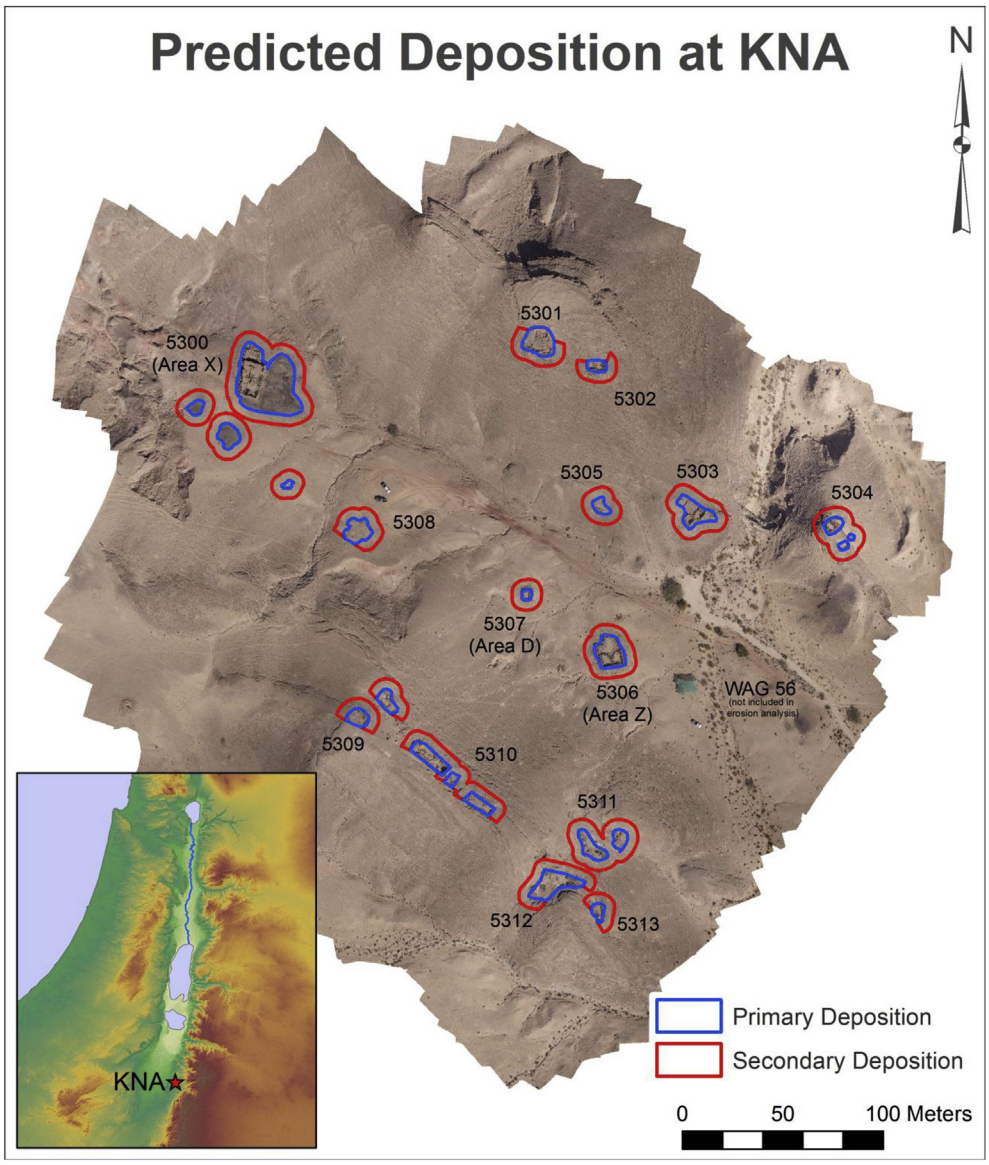

Fig. 3. Orthophoto of KNA with measured primary deposition and estimated secondary deposition. The inset map shows KNA's location in the southern Levant, 30 km southeast of the Dead Sea.

$$A = (R)(K)(LS)(C)(P)$$
$$A = (46.182)(0.52)(LS)(1)(1)$$

Fig. 4. The RUSLE Formula (Goldman et al., 1986: 5.2) and the calculated variables at KNA. *LS* refers to the LS-factor raster calculated across the site.

factor is fundamentally a measure of the degree of which slope length and gradient affect erosion, and as such, it was necessary to calculate these values across the site. To calculate the slope gradient across KNA, we applied the Slope tool in the Spatial Analyst toolbox (ESRI, 2013) to create a raster dataset with slope data at the site. In order to quantify slope length, we applied the Flow Length tool, also in the Spatial Analyst toolbox. This tool automatically calculates the distance downhill from local maximums to each cell at the site (ESRI, 2013), deriving a seamless slope length dataset. The last variable required to calculate the LS is known as the "m-factor," which consists of fixed values for ranges of slope. This we operationalized in GIS through reclassification (ESRI, 2013) of the slope raster. With each of the key variables for working out the LS-factor in raster format in GIS, we were able to implement the formula provided by Goldman et al. (1986: 5.20) into the raster calculator (Fig. 5) and create a raster dataset of the LS-factor over the entire site of KNA.

Calculation of the C- and P-factors was straightforward—as there are no cropping or conservation factors acting on the site,

$$LS = \left(\frac{65.41 \cdot s^2}{s^2 + 10{,}000} + \frac{4.56 \cdot s}{\sqrt{s^2 + 10{,}000}} + 0.065\right)\left(\frac{l}{72.5}\right)^m$$

```
LS = (((65.41 * ("Slope" ^ 2)) / (("Slope" ^ 2) + 10000)) + ((4.56 *
"Slope") / (SquareRoot(("Slope" ^ 2) + 10000)) + .065) *
((("FlowLength") / 72.5) ^ ("Mfactor")))
```

Fig. 5. The formula to calculate the *LS*-factor (Goldman et al., 1986: 5.20) and its operationalization in the ArcGIS Raster Calculator to calculate *LS* across the entire site of KNA.

these variables were assigned a value of 1 (Goldman et al., 1986: 5.22–24). With each of the variables involved in the RUSLE equation approximated or determined, we were able to calculate the equation within GIS by adapting the RUSLE formula from Goldman et al. (1986: 5.20) for use in the Raster Calculator in ArcGIS. This we accomplished by substituting the R-, K-, C-, and P-factors at KNA as sitewide constants into the equation, and multiplying these by the LS-factor raster already created (Fig. 4). This process allowed us to bring abstract (and not spatially-referenced) variables into our GIS and calculate erosion in tonnes/hectare/year across the site, with this data in spatially-referenced raster format. We reclassified this data according to previously-published erosion risk categories (Farhan et al., 2013) in Jordan in order to clearly understand the level of erosion risk across KNA and at different parts of the site (Fig. 6). One important aspect of the current study is that all of the RUSLE variables, with the exception of the slope-related LS factor, are considered as sitewide constants. This meshes with RUSLE's intended use for "specific field areas," (Wischmeier and Smith, 1978: 3), KNA's relatively small size (the site mainly consists of two slopes), and the lack of discernible soil type variation at the site. Thus, the results of the formula will vary as a function of slope across the site, reflecting the primacy of slope as a factor in erosion risk in small areas.

3. Results

3.1. Quantifying erosion

Our results show that the risk of erosion at KNA is very high (Fig. 5). 58.0% of the site is at either Severe (25–50 tonnes/hectare/year) or Extreme (>50 t/ha/yr) risk of erosion, with only 18.5% of the site at Minimal (0–5 t/ha/yr) or Low (5–15 t/ha/yr) risk. These findings — while striking — are not unexpected. Approaching the site, our team recognized that erosion could have had powerful effects on the formation of the site and distortion of archaeological context, because of the climatic and topographical conditions of the site. The site of KNA straddles a small valley, with structures perched on the top of steep hills on either side (see Fig. 1). Very

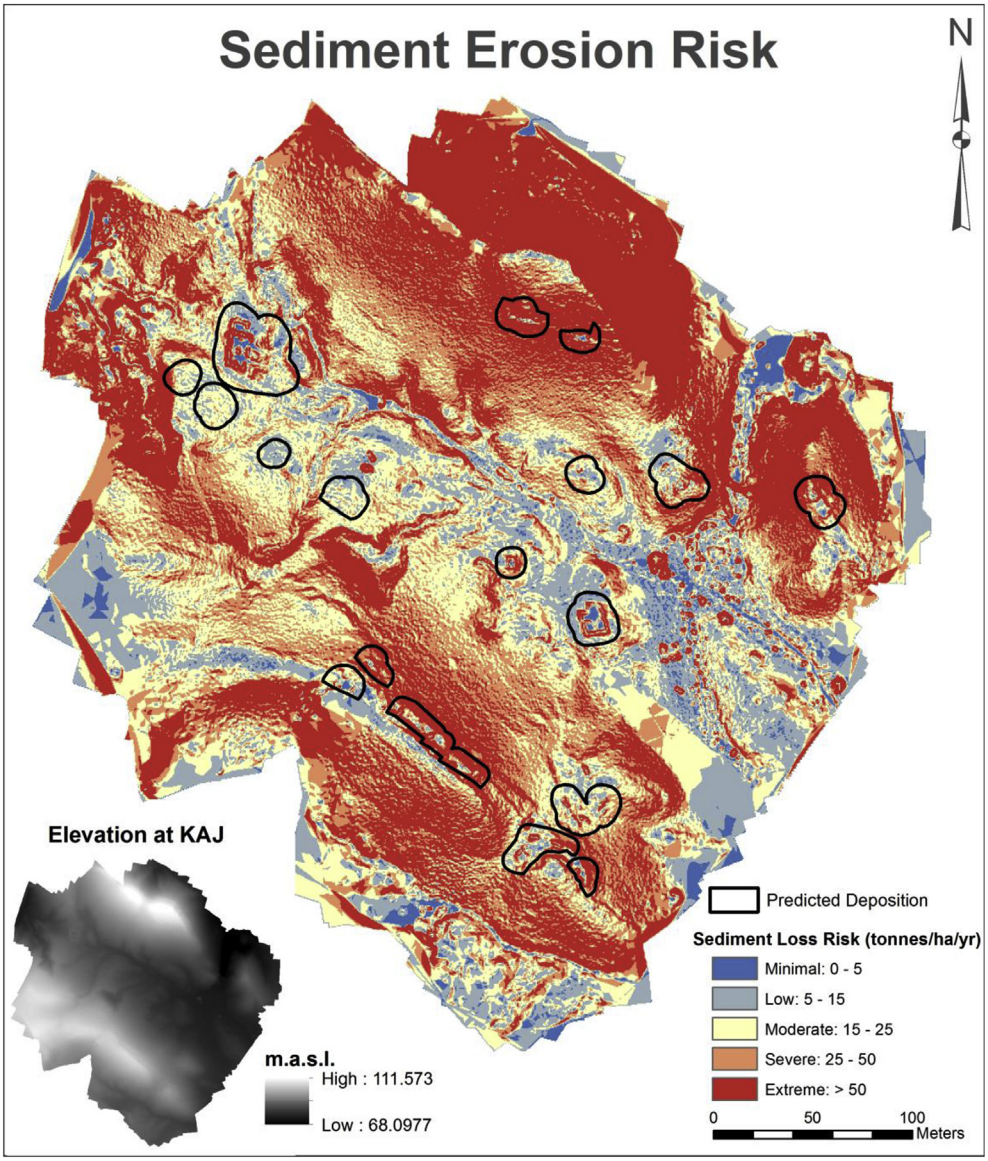

Fig. 6. RUSLE-based estimation of erosion risk at KNA in tonnes/hectare/year.

little sediment is actually present on the slopes of these hills, probably the result of erosion over time, corroborating the high predicted erosion risk at the site. In some areas of KNA, the sediment had completely eroded away and bedrock is present at the surface. Rain in the Faynan region of southern Jordan where KNA is located, when it does come, often occurs in intense storms that result in highly-erosive flash flooding events. Thus, affirmation that erosion may have had potentially severe effects on the site is not unexpected. Importantly, the RUSLE calculation predicts erosion risk, rather than actual erosion. Thus we should not expect that many tonnes of sediment will be removed from the slopes at KNA every year, but rather that what sediment is located in these higher-risk areas will be very likely to erode. Perhaps not coincidentally, the parts of the site calculated to have the highest erosion risk also have very little sediment present (as it is presumably continuously eroded away), whereas the lower-lying areas with lower erosion risk have accumulated more sediment. These results circumstantially support both the overall risk of erosion at the site and the patterning of erosion risk. Furthermore, pedestrian survey at KNA conducted in 2002 (Jones et al., 2012) and excavation in 2011 and 2012 add further circumstantial evidence to the risk of erosion at the site and reinforce the importance of spatial patterning. Circa 1300 ceramic sherds were collected from the surface at KNA, with hundreds of artifacts still visible at the site's surface, especially on slopes below structures. In contrast, only ca. 470 ceramic sherds were recovered from excavation of five structures at the site. One might reasonably expect these artifact distribution patterns to represent the results of erosional processes, given the demonstrated risk of erosion at the site.

3.2. Patterning of erosion

3.2.1. Background: patterning of erosion

While quantifying erosion risk at KNA was a satisfying first step in discovering the effects of this environmental formation process at the site, it provides only limited insight into the spatial patterning of the distortion erosion causes. Formation processes have predictable effects, and by understanding these processes, we can correct the distortions they introduce (Schiffer, 1972:677). Thus it is important to go beyond merely estimating the severity of erosion to actually begin to understand the patterning the process introduces. Data acquired through LAAP and IBM methods again proved useful to that end, in combination with data derived from other sources. The following analysis combines ethnoarchaeological data on the spatial patterning of deposition with GIS-based analysis to model the ways in which the archaeological record is altered and distorted by processes of erosion.

We relied on data derived from ethnoarchaeological study to create a model of depositional processes at sites. Schiffer (1972:161) differentiation between primary and secondary refuse is relevant here, although it bears some elaboration as to how elements are actually discarded, which led us to turn to the ethnoarchaeological data for specifics. Perhaps obviously, ethnoarchaeological studies indicate that central activity and habitation areas within structures in sedentary settlements are kept relatively clear of refuse in nearly all cases (Murray, 1980). These areas of active and frequent use are often swept to clear refuse (Simms, 1988), and the primary deposition (i.e. in their activity area) of elements in areas that are well-maintained is rare (LaMotta and Schiffer, 1999). As such, these areas have very little pottery when in active use (Longacre, 1981). Secondary discard is more complex than primary deposition, due to the fact that artifacts resulting from secondary disposal are removed from the location of their use. Deal (1985) provides a four-type schema of secondary discard: provisional discard, disposal resulting from household maintenance, dumping, and loss. Provisional discard refers to the stashing of broken elements so that they may be used later or collected for secondary disposal, and usually occurs in areas within or near living quarters. These areas are out of the way but readily accessible, including along interior walls, in corners, and also along exterior walls and fences (Hayden and Cannon, 1983; Deal, 1985). Provisional discard occurs in communities around the world, including Mayan households, Syrian villages, and semi-nomadic Bedouin camps in Jordan (Hayden and Cannon, 1983; Kamp, 2000; Simms, 1988). The second type of secondary element deposition is related to standard household maintenance, resulting in the relative cleanliness of activity areas. Various ethnographic sources evidence the processes of household cleaning (Simms, 1988; Binford, 1978; Longacre, 1981; Hayden and Cannon, 1983; Deal, 1985). Interestingly, some sources indicate an extremely casual attitude toward disposal of ordinary trash. This type of refuse can be swept or thrown out an entrance (Simms, 1988; Hayden and Cannon, 1983). Little effort is spent to dispose of animal bones or other organic refuse, other than to make sure it is disposed of in a downhill direction when a structure is on a slope (Hayden and Cannon, 1983). Dumping is Deal (1985) third form of secondary refuse disposal and it is responsible for the highest quantity of elements in the archaeological record. This type of deposition refers to elements that are intentionally discarded in a specific area. These areas need not be specific dumps, but can also be discard areas within household compounds or elsewhere (Deal, 1985). How to interpret high-density deposits such as pits has been an important matter of consideration (Wilson, 1994), although the study of such deposits depends on their discovery. Generally, ethnoarchaeological evidence suggests that the vast majority of refuse is actually deposited within compounds, or within concentrations of population (Murray, 1980; Hayden and Cannon, 1983). As Kamp (2000: 91) succinctly puts it, “few usable items reach the garbage dump.” Thus, between provisional discard, household maintenance disposal, and certain dumping processes, it seems that areas immediately inside (i.e. along walls) and nearby outside residences are some of the most critical for understanding sites during their period of active use. The spatial boundaries of the area of highest disposal density are somewhat flexible, given that household compound areas of varying sizes are the key loci of discard. However, based on certain ethnographic studies, it appears that a radius of approximately 5 m around households and key structures and activity areas is a common disposal pattern across various societies (Hayden and Cannon, 1983; Simms, 1988). Thus it seems that the highest density loci of secondary refuse disposal are often within 5 m of residences or locations at which activities are performed, with refuse not discarded directly uphill from these areas. These analogies are most appropriate for application to non-industrial areas at KNA (the majority of the structures at the site did not serve an industrial purpose). In the case of industrial areas at the site (Building 5300 in Area X, Building 5306 in Area Z, and Building 5304), an analogy derived from the excavation by ELRAP of structures related to the copper industry since 1999 is more directly appropriate. At other copper production sites in Faynan, where erosion is likely a lesser factor due to less varied topography, the highest density of industrial artifacts have been primarily recovered from within structures or slag mounds. The quantity of artifacts found outside these activity areas rapidly diminishes as a function of distance. For this reason, we decided to also apply the same 5 m deposition assumption to industrial areas at the site.

3.2.2. Methods: patterning of erosion

With a site-wide orthophoto derived from LAAP and IBM, it was a relatively simple process to operationalize these ethnographic and archaeological data into a hypothesis on artifact deposition at

the site of KNA. The ELRAP team identified structures, slag mounds, and activity areas at the site through a combination of pedestrian survey (Jones et al., 2012) and inspection of aerial imagery. These locations, representing areas of primary deposition and likely some provisional discard, were manually digitized as shapefiles in ArcGIS. Vector digitization of these areas was a key first step, facilitating the performance of more advanced forms of spatial analyses. These included simulating areas of high-density secondary deposition at the site. Given that the ethnographic data indicate the majority of secondary deposition (excluding dumping) takes place within 5 m of activity areas and residences, we buffered each of the digitized activity areas by 5 m, removing areas directly uphill from the activity areas. The results of this buffering (seen in Fig. 3) we regard as a hypothesis for the main locations of artifact deposition during the site's use.

Hypothesizing the spatial distribution of artifact deposition at KNA allows us to also predict the ways in which erosion might scatter these artifacts. Thus we aim to factor in both cultural and environmental formation processes in how we understand the creation and transformation of the archaeological record. Our simulation of the results of erosion relies on cost-path analysis, available as part of the Spatial Analyst toolbox in ArcGIS. Using the polygons representing each deposition area as origin points for least-cost paths down the slopes of the side, we calculated the paths of least resistance water and water-caused erosion would be likely to take down the slope for each area based on the DEM from LAAP and IBM data (First it was necessary to fill depressions resulting from noise in the DEM data (sinks), and subsequently derive a flow direction raster dataset from the DEM). The result of the cost path analysis — in raster format — was converted to polyline vector format in order to ease subsequent analysis. We then buffered the least-cost path polyline running down the slope by 5 m to represent a more realistic flow of water and to reflect the assumption that water flow in rainstorms will not strictly follow the most ideal path. These buffered pathways represent our hypothesis as to the most probable routes of erosion from each of the activity areas identified at the site. Because of the layout of the site, many of the calculated paths of erosion converge in the center of the site, in the wadi running through the site's center. Thus we chose to identify the paths corresponding to each activity area with different symbology, separating areas relating to more than one activity area. Fig. 7 displays the areas of simulated deposition in dark colors, with the associated areas that we predict artifacts might be deposited in by erosion represented in similar but lighter colors to represent that these areas are.

3.2.3. Results: patterning of erosion

The regions down-hill from each activity area represent our best estimate as to where the highest density of material eroded from its original context. Areas shown in lighter colors represent slopes directly downhill from activity areas, while parts of the site downslope from multiple activity areas, and thus with presumably mixed origins are shown in white (Areas not colored also represent unknown or mixed origins). Unfortunately, our ability to quantitatively assess the accuracy of these predictions is limited, as artifacts on the suface downslope from activity areas are without concrete context and their original provenience is unknown. However, exactly because these artifacts found on the surface are already deprived of most of their value in spatial context, any possibility of restoring some analytical value to these sherds should be embraced. As such, it may be possible to provisionally re-associate some of the surface artifacts with their original contexts, since we have generated predicted areas where the material would end up after eroding down the slope from activity areas. This may be important at sites like KNA, which has relatively few artifacts in secure archaeological contexts while many artifacts are recoverable from the surface of the site. By collecting surface artifacts but not attempting to establish their original contexts, archaeologists may be ignoring information that can potentially be of value to their research. Conversely, the possibility of re-associating artifacts with lost contexts through modeling and understanding of site formation processes may provide a new way for scholars to understand their sites at a deeper level and uncover new information about the past.

3.2.4. Comparison of results to the study to previous excavations at surveys

The accuracy of the erosional deposition model presented in Fig. 7 can be tested against the results of the 2002 survey of the site and excavations in 2011 and 2012 (Areas and building numbers shown in Fig. 3). The model is in general agreement with these results, and helps explain several initially confusing phenomena. In Buildings 5301 and 5302, the survey collection supports the model's prediction of severe to extreme erosion. Between both buildings, only 20 sherds were collected, with the vast majority coming from inside the walls of 5301. Although systematic collection did not occur on the slope below, four glazed sherds were collected near the wadi, and likely eroded from one of the two buildings. The model predicts more moderate erosion from Building 5303 (excavation Area Y), but the 2002 survey collected only 64 sherds in this building and the 2012 excavations reached bedrock after little more than 0.25 m. The excavations, however, also recovered 46 sherds from a 7 m^2 probe, some of them belonging to relatively complete vessels with well-preserved decoration. Given that the model predicts less erosion in this area than surrounding areas, the shallowness of the sediments here may be related to a lack of post-abandonment deposition, rather than erosion of those sediments, but modeling of aeolian processes at the site would be necessary to test this assumption. In the southern part of the site, severe to extreme erosion would also be predicted for Building 5310 (excavation Area A). While 104 sherds were collected from this building during the 2002 survey, this must be considered in relation to the size of the building, which stretches across ca. 90 m of hillside. The 2012 excavations reached bedrock after only 0.5 m, and recovered only 24 sherds from a 24 m^2 square, suggesting that erosion has been as substantial as predicted by the model. In the site's central valley, only low to moderate erosion would be expected for Building 5306 (excavation Area Z). 190 sherds were collected from this area during the 2002 survey, and the excavation recovered 297 sherds from a 52.5 m^2 area. Most interesting is Building 5307 (excavation Area D), a small (ca. 5×4 m) building northwest of Area Z. The 2002 survey collected 68 sherds from this building, which is fairly high, as Area D is the smallest preserved structure at the site. A 2×1 m probe was excavated during the 2012 season, and only five sherds were recovered, however. The model helps explain this discrepancy, as erosion of material from Area A into Area D is also expected. As such, many of the ceramics collected outside of Area D during the 2002 survey should actually be attributed to Area A, which explains the presence of wheel-made and mold-made types not found in the Area D probe. A final interesting point concerns WAG 56, a cemetery site in the valley below the Building 5311–5313 complex (n.b.: this site is not included as a depositional area in the analysis here). 176 Middle Islamic period sherds were collected at this site during the 2002 survey, which is more than would be expected for a site consisting of only 8–10 burials, and Jones et al. (2012: 79) note that, at the time, they were uncertain whether these sherds should be associated with the burials or with KNA. The model, which predicts severe erosion from the Building 5311–5313 complex into the valley below, helps resolve this question. Many, if not all, of the Middle

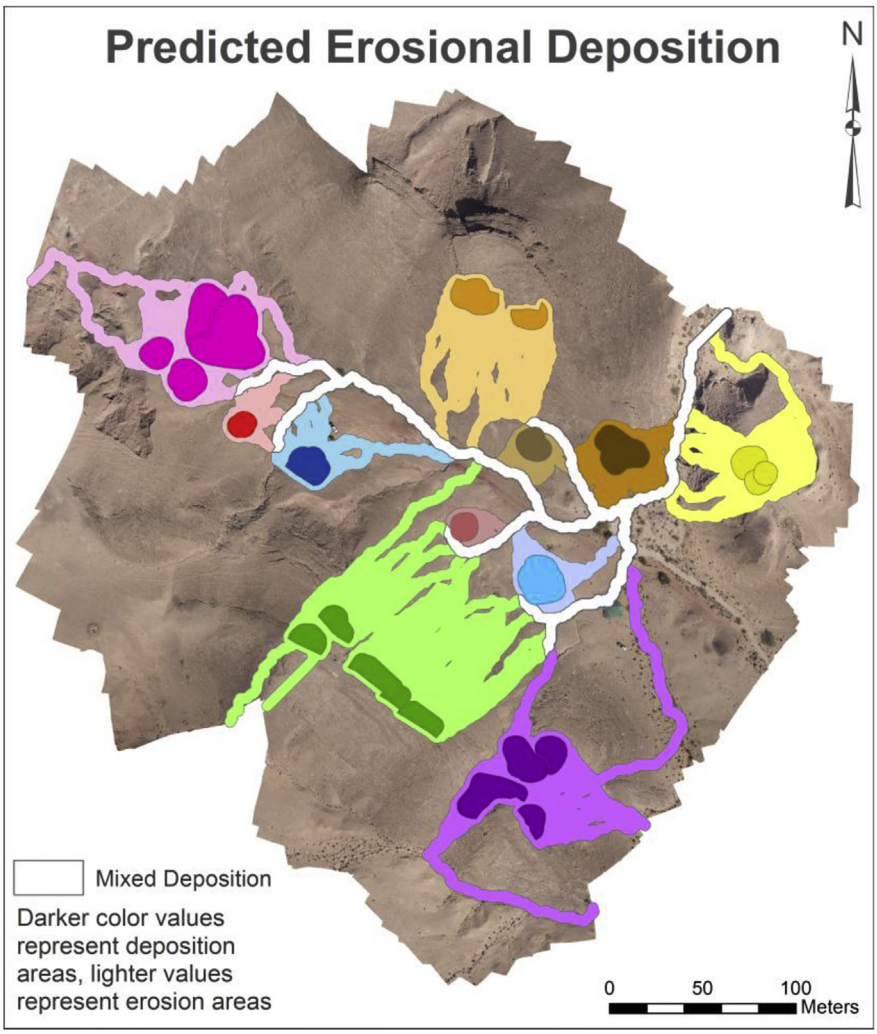

Fig. 7. Estimated deposition from erosion at the site. The darker colors in the image represent areas of estimated primary and secondary deposition. Associated lighter colors represent our hypothesis of where artifacts may have been deposited by erosion. (For interpretation of the references to color in this figure legend, the reader is referred to the Web version of this article.)

Islamic sherds from WAG 56 likely eroded from the KNA hillside above.

4. Discussion

The combined methods of LAAP and IBM serve as an excellent basis for the acquisition of high-resolution spatially-referenced data with a minimum of time spent in the field. These data, in turn, allow for the performance of complex spatial analyses at an intra-site scale. Given that satellite data is usually not of a sufficient resolution to conduct analysis within the framework of a site, the outputs generated by these methods represent a significant advancement over those from previously-available technology. The importance of the effects of natural processes on the archaeological record is not a novel concept, yet the effects of water-based erosion on artifact distribution patterns have (in our view) been under-studied. We believe that an *a priori* consideration of the effects of water-caused erosion can be both necessary and beneficial to archaeological investigation. As we have seen, it can both clear up the relationship between systemic and archaeological context and potentially even re-associate artifacts with their original contexts in a provisional way. Thanks to modern technology and techniques, we now have the potential to conduct more intra-site spatial analyses, including those relating to n-transforms. This type of study can potentially be a boon to archaeologists interested in understanding the development of their site over time and improving their understanding of the past.

Acknowledgements

Thanks to the UCSD Levantine and Cyber-Archaeology Laboratory, ELRAP staff and volunteers, and the locals of Qirayqira and Faynan for their invaluable assistance in completing this work.

Funding: This work was supported by the National Science Foundation under IGERT Award #DGE-0966375, "Training, Research and Education in Engineering for Cultural Heritage Diagnostics." Major funding came from TEL's Norma Kershaw Chair, Department of Anthropology and Judaic Studies, UCSD. Also, thanks to ACOR, Dr. M. Jamhawi, and the Department of Antiquities of Jordan.

References

Ben-Yosef, E., Levy, T.E., Higham, T., Najjar, M., Tauxe, L., 2010. The beginning of Iron Age copper production in the southern Levant: new evidence from Khirbat al-

Jariya, Faynan, Jordan. Antiquity 84, 724–746.
Binford, L., 1978. Dimensional analysis of behavior and site structure: learning from an eskimo hunting stand. Am. Antiq. 43 (3), 330–361.
Casler, C.L., 2006. Developing a Web Resource on Soils and Land Management in Jordan. Electronic document. http://cals-cf.calsnet.arizona.edu/ialc/ialc4.asp?proj=03D-02. (Accessed 5 February 2014).
Chen, H., El Garouani, A., Lewis, L.A., 2008. Modelling soil erosion and deposition within a Mediterranean mountainous environment utilizing remote sensing and GIS – Wadi Tlata, Morocco. Geograph. Helv. 63 (1), 36–47.
Cruz, F., Petit, C., Pertlwieser, T., Chaume, B., Mordant, C., Chateau, C., 2014. Erosion of the defensive system of the 'princely' site of Vix (France): a geoarchaeological approach. In: Meylemans, E., Poesen, J., In't Ven, I. (Eds.), Relicta Monografieën 9. The Archaeology of Erosion, the Erosion of Archaeology. Proceedings of the Brussels Conference, April 28-30 2008. Flanders Heritage Agency, Brussels, pp. 73–86.
De Reu, J., De Smedt, P., Herremans, D., Van Meirvenne, M., Laloo, P., De Clercq, W., 2014. On introducing an image-based 3D reconstruction method in archaeological excavation practice. J. Archaeol. Sci. 41, 251–262.
Deal, M., 1985. Household pottery disposal in the maya highlands: an ethnoarchaeological interpretation. J. Anthropol. Archaeol. 4, 243–291.
Doneus, M., Verhoeven, G., Fera, M., Briese, C., Kucera, M., Neubauer, W., 2011. From deposit to point cloud—a study of low-cost computer vision approaches for the straightforward documentation of archaeological excavations. Geoinformatics 6, 81–88.
ESRI, 2013. ArcGIS Help 10.1. Electronic document. http://resources.arcgis.com/en/help/main/10.1/index.html#/Raster_to_Polyline/001200000009000000/. (Accessed 3 February 2014).
Farhan, Y., Zregat, D., Farhan, I., 2013. Spatial estimation of soil erosion risk using RUSLE approach, RS, and GIS techniques: a case study of Kufranja watershed, Northern Jordan. J. Water Res. Protect. 5 (12), 1247–1261.
Forte, M., 2014. 3 D archaeology: new perspectives and challenges—the example of çatalhöyük. Journal of Eastern Mediterranean Archaeology and Heritage Studies 2 (2), 1–29.
Ganasri, B.P., Ramesh, H., 2016. Assessment of soil erosion by RUSLE model using remote sensing and GIS - a case study of Nethravathi Basin. Geoscience Frontiers 7 (6), 953–961.
Goldman, S.J., Jackson, K., Bursztynsky, T.A., 1986. Erosion & Sediment Control Handbook. McGraw-Hill Book Company, New York.
Hayden, B., Cannon, A., 1983. Where the garbage goes: refuse disposal in the maya highlands. J. Anthropol. Archaeol. 2, 117–163.
Hijmans, R.J., Cameron, S.E., Parra, J.L., Jones, P.G., Jarvis, A., 2005. Very high resolution interpolated climate surfaces for global land areas. Int. J. Climatol. 25, 1965–1978.
Howland, M.D., 2014. Structure from motion: twenty-first century field recording with 3D technology. Near E. Archaeol. 77 (3), 187–191.
Howland, M.D., Liss, B., Najjar, M., Levy, T.E., 2015. GIS-based mapping of archaeological sites with low-altitude aerial photography and structure from Motion: A case study from Southern Jordan. In: 2015 Digital Heritage, Granada, vol. 2015, pp. 91–94.
James, P.A., Mee, C.B., Taylor, G.J., 1994. Soil erosion and the archaeological landscape of methana, Greece. J. Field Archaeol. 21 (4), 395–416.
Jones, I.W.N., Levy, T.E., Najjar, M., 2012. Khirbat Nuqayb al-asaymir and Middle islamic metallurgy in faynan: surveys of Wadi al-ghuwayb and Wadi al-jariya in faynan, southern Jordan. Bull. Am. Sch. Orient. Res. 368, 67–102.
Jones, Ian W.N., Najjar, Mohammad, Levy, Thomas E., 2014. Not found in the order of history: toward a "medieval" archaeology of southern Jordan. In: Stull, S.D. (Ed.), From West to East: Current Approaches in Medieval Archaeology, pp. 179–205 (Newcastle-upon-Tyne: Cambridge Scholars).
Jones, I.W.N., Najjar, M., Levy, T.E., 2017. The Araba copper industry in the Islamic period: views from Faynan and Timna. In: Ben-Yosef, E. (Ed.), Mining for Copper: Environment, Culture and Copper in Antiquity, in Memory of Professor Beno Rothenberg. Tel Aviv University Institute of Archaeology, Tel Aviv in press.
Jorayev, G., Wehr, K., Benito-Calvo, A., Njau, J., de la Torre, I., 2016. Imaging and photogrammetry models of olduvai gorge (Tanzania) by unmanned aerial vehicles: a high-resolution digital database for research and conservation of early stone Age sites. J. Archaeol. Sci. 75, 40–56.
Kamp, K., 2000. From village to tell: household ethnoarchaeology in Syria. Near E. Archaeol. 63 (2), 84–93.
Lambers, K., Eisenbeiss, H., Sauerbier, M., Kupferschmidt, D., Gaisecker, T., Sotoodeh, S., Hanusch, T., 2007. Combining photogrammetry and laser scanning for the recording and modeling of the Late Intermediate period site of Pinchango Alto, Palpa, Peru. J. Archaeol. Sci. 34, 1702–1712.
LaMotta, V.M., Schiffer, M.B., 1999. formation processes of house floor assemblages. In: Allison, Penelope M. (Ed.), The Archaeology of Household Activities. Routledge, London, pp. 19–29.
Levy, T.E., Adams, R.B., Witten, A.J., Anderson, A., Arbel, Y., Kuah, S., Moreno, J., Lo, A., Wagonner, M., 2001. Early metallurgy, interaction, and social change: the jabal hamrat fidan (Jordan) research design and 1998 archaeological survey: preliminary report. Annu. Dep. Antiq. Jordan 45, 159–187.
Levy, T.E., Adams, R.B., Anderson, J.D., Najjar, M., Smith, N., Arbel, Y., Soderbaum, L., Muniz, A., 2003. An Iron Age landscape in the edomite lowlands: archaeological surveys along Wadi Al-Ghuwayb and Wadi Al-Jariya, jabel hamrat fidan, Jordan 2002. Annu. Dep. Antiq. Jordan 47, 247–277.
Levy, T.E., Ben-Yosef, E., Najjar, M., 2014b. The Iron Age edom lowlands regional archaeology project research, design, and methodology. In: Levy, T.E., Najjar, M., Ben-Yosef (Eds.), New Insights into the Iron Age Archaeology of Edom, Southern Jordan, vol. 1. The Cotsen Institute of Archaeology Press, University of California, Los Angeles, Los Angeles, CA, pp. 1–88.
Levy, T.E., Ben-Yosef, E., Najjar, M., 2014c. Excavations at Khirbat en-Nahas 2002-2009: an Iron Age Copper Production Center in the Lowlands of Edom. In: Levy, T.E., Najjar, M., Ben-Yosef (Eds.), New Insights into the Iron Age Archaeology of Edom, Southern Jordan, vol. 1. The Cotsen Institute of Archaeology Press, University of California, Los Angeles, Los Angeles, CA, pp. 89–246.
Longacre, W.A., 1981. Kalinga pottery: an ethnoarchaeological study. In: Hodder, I., Isaac, G., Hammond, N. (Eds.), Patterns of the Past: Studies in Honour of David Clarke. Cambridge University Press, Cambridge, pp. 49–66.
Meylemans, E., Poesen, J., In't Ven, I., 2014. Relicta monografieën 9. The archaeology of erosion, the erosion of archaeology. In: Proceedings of the Brussels Conference, April 28-30 2008. Flanders Heritage Agency, Brussels, pp. 73–86.
Murray, P., 1980. Discard location: the ethnographic data. Am. Antiq. 45 (3), 490–502.
Olson, B.R., Placchetti, R., Quartermaine, J., Killebrew, A.E., 2013. The tel akko total archaeology project (akko, Israel): assessing the suitability of multi-scale 3D field recording in archaeology. J. Field Archaeol. 38, 244–262.
Quartermaine, J., Olson, B.R., Killebrew, A.E., 2014. Image-based modeling approaches to 2D and 3D drafting in archaeology at tel akko and qasrin: two case studies. Journal of Eastern Mediterranean Archaeology and Heritage Studies 2 (2), 110–127.
Remondino, F., El-Hakim, S., 2006. Image-based 3D modelling: a review. Photogramm. Rec. 21 (115), 269–291.
Remondino, F., Barazzetti, L., Nex, F., Scaioni, M., Sarazzi, D., 2011. UAV photogrammetry for mapping and 3D modeling – current status and future perspectives. Int. Arch. Photogram. Rem. Sens. Spatial Inf. Sci. 38 (1).
Renard, K.G., Freimund, J.R., 1994. Using monthly precipitation data to Estimate the *R* factor in the revised USLE. J. Hydrol. 157, 287–306.
Renard, K.G., Laflen, J.M., Foster, G.R., McCool, D.K., 1994. The revised universal soil Loss equation. In: Lal, R. (Ed.), Soil Erosion Research Methods, second ed. St. Lucie Press, USA, pp. 105–124. Soil and Water Conservation Society.
Reshetyuk, Y., Mårtensson, S.G., 2016. Generation of highly accurate digital elevation models with unmanned aerial vehicles. Photogramm. Rec. 31 (154), 143–165.
Roosevelt, C.H., 2014. Mapping site-level microtopography with real-time kinematic global navigation satellite systems (RTK GNSS) and unmanned aerial vehicle photogrammetry (UAVP). Open Archaeol. 1, 29–53.
Sapirstein, P., 2016. Accurate measurement with photogrammetry at large sites. J. Archaeol. Sci. 66, 137–145.
Schiffer, M.B., 1972. Archaeological context and systemic context. Am. Antiq. 37 (2), 156–165.
Simms, S.R., 1988. The archaeological structure of a Bedouin camp. J. Archaeol. Sci. 15, 197–211.
Smith, N.G., Passone, L., al-Said, S., al-Farhan, M., Levy, T.E., 2014. Drones in archaeology: integrated data capture, processing, and dissemination in the al-ula valley, Saudi Arabia. Near E. Archaeol. 77 (3), 176–181.
Smith, N.G., Howland, M., Levy, T.E., 2015. Digital archaeology field recording in the 4th dimension: ArchField C++ a 4D GIS for digital field Work (in press). In: Proceedings of the 2015 Digital Heritage International Congress, pp. 1–9.
Stiros, S.C., Barkas, N., Moutsoulas, M., 1999. River erosion and landscape reconstruction in Epirus: methodology and results. British school at Athens studies. In: The Palaeolithic Archaeology of Greece and Adjacent Areas: Proceedings of the ICOPAG Conference, Ioannina, September 1994, vol. 3, pp. 108–114.
Taguas, E.V., Cuadrado, P., Ayuso, J.L., Yuan, Y., Pérez, R., 2010. Spatial and Temporal evaluation of erosion with RUSLE: a case study in an olive orchard microcatchment in Spain. Solid Earth Discuss 2, 275–306.
Thomas, H. A methodology for combining terrestrial and aerial photographs to create high resolution photogrammetric models of large-scale archaeological sites: a case study for Methone, Greece, J. Agric. Soc. Res. 16 27–33.
Turnbaugh, W.A., 1978. Floods and archaeology. Am. Antiq. 43 (4), 593–607.
Ullman, S., 1979. The interpretation of structure from motion. Proc. Roy. Soc. Lond. 203 (1153), 405–426.
Verhoeven, G., 2011. Taking computer vision aloft – archaeological three-dimensional reconstructions from aerial photographs with PhotoScan. Archaeol. Prospect. 18 (1), 67–73.
Verhoeven, G., Taelman, D., Vermeulen, F., 2012. Computer vision-based orthophoto mapping of complex archaeological sites: the ancient quarry of pitaranha (Portugal-Spain). Archaeometry 54 (6), 1114–1129.
Wainwright, J., 1994. Erosion of archaeological sites: results and implications of a site simulation model. Geoarchaeology 9 (3), 173–201.
Wilson, D.C., 1994. Identification and assessment of secondary refuse aggregates. J. Archaeol. Meth. Theor 1 (1), 41–68.
Wischmeier, W.H., Smith, D.D., 1965. Predicting Rainfall Erosion Losses from Cropland East of the Rocky Mountains, Agriculture Handbook No. 282, U.S. Department of Agriculture, Washington, D.C.
Wischmeier, W.H., Smith, D.D., 1978. Predicting Rainfall Erosion Losses: a Guide to Conservation Planning. U.S. Department of Agriculture, Agriculture Handbook No. 537.
Wischmeier, W.H., Johnson, C.B., Cross, B.V., 1971. A soil erodibility nomograph for farmland and construction sites. J. Soil Water Conserv. 26, 189–192.
Yoon, K.S., Kim, C.W., Woo, H., 2009. Application of RUSLE for erosion estimation of construction sites in coastal catchments. J. Coast Res. (56), 1696–1700.